Steering the Dynamics within Reduced Space through Quantum Learning Control

Young Sik Kim

Department of Science, Hongik University, Seoul 121-791, Korea
Received March 3, 2003

In quantum dynamics of many-body systems, to identify the Hamiltonian becomes more difficult very rapidly as the number of degrees of freedom increases. In order to simplify the dynamics and to deduce dynamically relevant Hamiltonian information, it is desirable to control the dynamics to lie within a reduced space. With a judicious choice for the cost functional, the closed loop optimal control experiments can be manipulated efficiently to steer the dynamics to lie within a subspace of the system eigenstates without requiring any prior detailed knowledge about the system Hamiltonian. The procedure is simulated for optimally controlled population transfer experiments in the system of two degrees of freedom. To show the feasibility of steering the dynamics to lie in a specified subspace, the learning algorithms guiding the dynamics are presented along with frequency filtering. The results demonstrate that the optimal control fields derive the system to the desired target state through the desired subspace.

Key Words : Quantum learning control, Optimal control experiment, Quantum dynamics

Introduction

During the last decade, quantum molecular control has been studied for designing optical control field to actively manipulate quantum dynamical system.[1-3] Similar logic has been applied to designing laser pulses to drive other dynamical processes including solid-state applications.[4] Optimal control theory (OCT) lends itself to a systematic search for the control functions or parameters to achieve a prescribed physical goal while also avoiding deleterious processes. However, especially for polyatomic molecules, this open-loop OCT has a number of serious problems: (a) the Hamiltonian is only approximately known, (b) the design equations for complex systems will likely call for approximate solutions, and (c) the field designs produced in the laboratory may have systematic and random errors.[5] Thus, this situation points to the need for closing the loop in the laboratory by Optimal control experiment (OCE).[6]

The OCE search the optimal control field by learning from the previous trials through closed-loop procedures until one that derives the system to the desired target is achieved while also avoiding deleterious processes. At each loop in the search, the measured outcomes from previous trials are used to select the new test field using an optimization procedure based on a genetic[7,8] or gradient algorithm until sufficient control is achieved. Such a method is appealing because it requires no previous information about the system Hamiltonian, although convergence would surely be improved by utilizing available Hamiltonian structure. Thus, the OCE closed-loop process eliminates issues of Hamiltonian uncertainty. Also, the OCE does not need to solve Schrodinger's equation because of the actual molecules and their dynamics are part of the loop. The closed loop OCE technique can be applied to seek control of systems having an arbitrary number of the degrees of freedom.

The successful OCE control has been carried out in a wide variety of systems with the goal of generating a particular optical pulse shape recently.[9-17] Wilson *et al.* manipulated the emission of a laser dye using laser chirp control knobs,[10] and Gerber *et al.* used laser phase modulation to control the ratios of the products in the fragmentation and ionization of two organometallic compounds.[11] The experiments by Meshulach and Silberberg demonstrate that OCE can be effective for learning two-photon atomic level population control.[14]

However, in practice, application of the closed-loop learning procedure become more difficult very rapidly as the number of degrees of freedom increases by the difficulty of finding a global minimum. Thus, it is of considerable interest to develop a constrained OCE procedure, which steers the dynamics to lie in a specified subspace or on a subset of the most desired subsystem Hamiltonian. For inversion of molecular Hamiltonian information, it may also be very attractive to use the closed loop learning procedure.[18] The difference between OCE and the inversion procedure are as in the case of inversion, the Hamiltonian such as the dipole moment or the potential energy surface are not known beforehand. Nevertheless, the closed loop OCE procedure appears feasible for learning about molecular Hamiltonians and Figure 1 illustrates the components involved. In order to deduce dynamically relevant Hamiltonian information, it is desirable to control the dynamics to lie within a reduced domain. After the i-th loop, the molecular observation updates the inverted Hamiltonian informations, as well as provides an estimate for the reduced domain stability where the Hamiltonian information may be reliably extracted. The learning algorithm generating the laser field operates to ensure that dynamics remain in the reduced domain and the stability of the domain can control the quality of the inverted Hamiltonian informations.

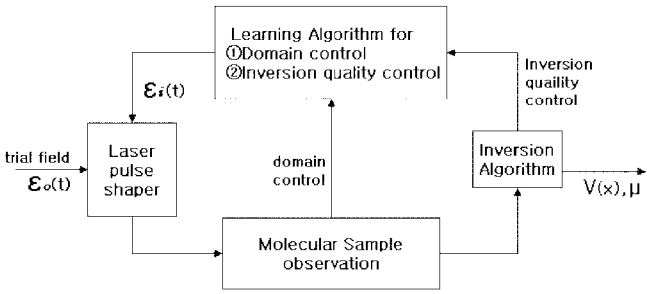

Figure 1. Closed loop process for learning control of molecular Hamiltonian information. The learning algorithm serves the purpose of guiding the control field to maintain the dynamics in a specified subspace as well as to control the inversion quality of the Hamiltonians by the domain stability.

A recently introduced tracking approach can achieve a form of reduced space dynamics by a priori specifying an objective trajectory track as the expectation values of a chosen operator.[19] The technique deduces the control electric field such that the system evolution exactly follows the temporal track. This approach has certain attractive features, but presently the choice of the expectation values is a heavy demand calling for the considerably physical insight. Another approach of a reduced description of the dynamics focuses on a subset of the most important degrees of freedom and treats the other degrees of freedom as a background to which the subset is coupled.[20] However, this reduction is useful only if it suggests accurate approximations which permit analysis of the dynamics of the subsystem with weak perturbations from the background.

In this paper, we introduce a constrained OCE that greatly simplifies the dynamics without a priori specifying an trajectory track. Only minimal information is needed about the system states or other characteristics to specify a subspace of interest for the dynamics to reside in. This freedom of manipulation permits the actual dynamical path to evolve unconstrained within the subspace. The price paid for seeking this reduction of the dynamics is the need to perform an extra set of temporal observations as data for the learning algorithm to guide the dynamics so that it stays within the subspace. This paper will introduce OCE reduced space dynamics through simple modifications of the cost functional as part of the learning algorithm. In Sect. II, the OCE formulation for the steering the dynamics within reduced space is presented, and section III demonstrates simulated application of this algorithm to complex systems and illustrates a tailored cost functional to steer dynamics that greatly simplifies the complexity of the system Hamiltonian. Closed-loop process for learning molecular Hamiltonian is discussed.

Reduced Space Optimal Control Experiment

To steer the dynamics to lie within a specified subspace by tailored cost functionals, we simulated constraint OCE procedure involving population transfer in multi-level quantum systems. The physical system has N levels radiatively connected by up to L transitions. The Hamiltonian that describes these N eigenstates of the molecule is

$$H_0 = \sum_{i=0}^{N-1} E_i |\phi_i\rangle\langle\phi_i| \tag{1}$$

where E_i is the energy of eigenstate $|\phi_i\rangle$. The interaction between the molecule and the field is described by the time dependent Schrodinger equation with the initial wavefunction $|\Psi(0)\rangle$ containing all population in the ground state.

$$\frac{\partial}{\partial t}|\Psi(t)\rangle = -i[H_0 - \mu\varepsilon(t)]|\Psi(t)\rangle \tag{2a}$$

$$|\Psi(0)\rangle = |\phi_0\rangle \tag{2b}$$

and the control field is a modulated Gaussian given by,

$$\varepsilon(t) = \exp[-(t-T/2)^2/(2s^2)] \sum_{l}^{L} A_l \cos(\omega_l t + \theta_l) \tag{3}$$

where the ω_l are the transition frequencies of the system, and the A_l and θ_l are the corresponding amplitudes and their associated phases, respectively. In the present closed loop learning control experiments, it is desired to pump all population from the ground state to the i-th population P_i^T at the target time T , in an efficient manner by eliminating the insignificant field components and by guiding the dynamics to lie in a specified subspace. Also, the cost functional guiding the experiments can contain only quantities which may be explicitly measured. Thus, the physical objective functional is specifically given by,

$$J[\Psi(t), \varepsilon(t)] = \Phi(T) + L_1 + L_2 + L_3 \tag{4}$$

with

$$\Phi(T) = \sum_{i}^{N} [P_i(T) - P_i^T]^2 \tag{5a}$$

$$L_1 = \beta_1 \sum_{l} A_l^2 \tag{5b}$$

$$L_2 = \beta_2 \sum_{l} \theta_l^2 \tag{5c}$$

$$L_3 = \beta_3 \int_0^T dt \sum_{j}^{N-N'} P_j(t). \tag{5d}$$

The learning algorithm in the closed loop works to find a control field $\varepsilon(t)$ that minimizes the objective functinal J. The error function $\Phi(T)$ in Eq. (5a) serves to transfer the i-th state actual population $P_i(t)$ toward the desired population P_i^T by the field at the target time T. While Eq. (5b) and Eq. (5c) contain the positive field cost functions which is dependent on the amplitudes and phases of the field. These terms minimize all the amplitudes and phases of the field components that have little significance for the controlled dynamics. In general, it is not necessary to have all frequency and phase components for achieving control, especially, for steering the dynamics to lie in a specified

subspace. One or more frequencies might have little effect on the subspace. Thus, the extraneous frequencies should be suppressed down especially in reducing the space dynamics on a desired subsystem Hamiltonian. This is coincident with current pulse shaping technology operating in the frequency domain and the associated control knobs are the amplitudes and phases at a set of discrete field frequencies.

The cost function L_3 in Eq. (5d) are explicitly present to guide the dynamics to lie in a subspace. In the present context a subspace is defined to consist of a subset of N' states drawn from the full set with $N' < N$. This term aims to keep population out of the undesirable $N-N'$ states throughout the control time interval $0 \le t \le T$. An observation of $P_j(t)$ for these $N-N'$ states is needed to evaluate this term. The positive weights β_1, β_2 and β_3 in Eqs. (5b-5d) balance the contributions of the various cost terms. In certain circumstances simply filtering out certain frequency components will serve to restrict the dynamics to lie within the N' eigenstates of the field free Hamiltonian H_0. Frequency filtering can be effective when the states within the desired subspace have clearly distinct transition frequencies amongst themselves which are separate from those connecting to the states outside of the subspace. If frequency filtering alone achieves the control objective along with confinement of the dynamics to the desired subspace, then no additional observations are needed. However, in general the population dependent term weighted by β_3 will be required to attain this extra goal, and additional observations will be needed.

In the current closed-loop experiments, the OCE cost functional only explicitly contained in Eq. (5a) and Eq. (5d), and implicit costs on the field were borne by constraints inherent in the laser apparatus. Thus, the constant amplitude A_l and phase θ_l are parameters of the field are optimized because the system transition frequencies can be obtained from the spectroscopic data. For computational convenience, the optimization is performed with respect to the parameters b_l and c_l which are related to the experimental field parameters by $A_l^2 = b_l^2 + c_l^2$ and $\theta_l = \arctan(c_l/b_l)$. Optimizing the b_l and c_l parameters instead of the amplitude and phase parameters was found to be convenient because the amplitudes A_l are automatically restricted to non-negative values and the phases are automatically restricted to the range $[-\pi, \pi]$ but the range of the optimizing b_l and c_l parameters is unrestricted.

The three basic components of the OCE algorithm are the laser system which generates a known field that is applied to the molecular system, a detector which records the response of the system to the field, and computer coded logic to optimize the field using the field and response data. Here we employ a gradient-based algorithm for the optimization, although the genetic algorithm or even others could be employed. An outline of the algorithm is as follows:

1. Choose appropriate cost functional, which are functions of detectable observables, and applied the initial guess field to the system, record the detector response and compute the objective functional J.

2. Increase the field parameter b_l (or c_l), as $b_l \rightarrow b_l + \delta b_l$ (or $c_l \rightarrow c_l + \delta c_l$) with the initial value of the constant $\delta = 0.01$ used to increment the control parameters b_l (or c_l) for gradient computations while all other field parameters remain unchanged. Using the new parameters, apply the new field to the system; record the detector response and compute a new objective functional J'.

3. If there is no discernable difference between J and J', then increase δ by a factor 1.5 and go back to step 2.

4. Repeat step 2 and 3 for the remaining field parameters b_2, ... b_L and c_1, ... c_L.

5. Directly compute the gradient g_l for each field parameter b_l and c_l : $g_l = (J' - J)/\delta b_l$ and $g_{L-l} = (J' - J)/\delta c_l$; normalize the gradient g_l for each field parameter.

6. Modify the original field using a gradient-based optimization procedure: $b_l^{new} = b_l^{old} - \alpha g_l$ and $c_l^{new} = c_l^{old} - \alpha g_{L+l}$, where α is a small positive number for the smooth descent into the objective functional minimum.

7. Repeat steps 2-6 until convergence is attained.

The simulations of the experiments in this work include the frequency filtering to reduce the number of state. We define the transition frequency component in Eq. (3) that is associated with a desired pathway or an undesired pathway. The outline of the filtering algorithm is same as previous case except the pathway restriction is setting on the gradient in step 5, instead of the extra cost functional in step 1. The filtering gradient computed from the gradient g_l multiplied by a filtering factor f_l as $g_l^{filter} = g_l \times f_l$. If ω_l is related with undesirable state, $f_l = 0$, otherwise $f_l = 1$. The filtering algorithm is simple and very successful in a simple case, however, it can not be applicable in the cases of spectral congestion.

Illustration of Steering the Dynamics

This section will use simulations to explore the ability of the cost in Eq. (4) to steer population to a target state while simultaneously keeping the dynamics in a specified reduced dimensional space. Naturally the subspace must contain the initial and final states. The illustrations aim to show the feasibility of steering the dynamics to lie in a specified subspace by the constraint OCE procedure along with frequency filtering. The model systems have two degrees of freedom with the eigenstates of the field free Hamiltonian H_0 being $|v_1, v_2\rangle$ where the quantum numbers take on the values $v_i = 0, 1, 2, 3$. The system has 16 states with the following allowed transitions: $|v_1, v_2\rangle \leftrightarrow |v_1+1, v_2\rangle$, $|v_1, v_2\rangle \leftrightarrow |v_1+2, v_2\rangle$, $|v_1, v_2\rangle \leftrightarrow |v_1, v_2+1\rangle$, $|v_1, v_2\rangle \leftrightarrow |v_1, v_2+2\rangle$ and $|v_1, v_2\rangle \leftrightarrow |v_1\pm1, v_2\pm1\rangle$. The double headed arrows imply that excitation and de-excitation may occur, and in the case $|v_1, v_2\rangle \leftrightarrow |v_1\pm1, v_2\pm1\rangle$ the transitions involving the two states can occur independently. The transition frequencies associated with the individual quantum states will be denoted respectively as $\omega^1_{v_1v_1'}$ and $\omega^2_{v_2v_2'}$ while the simultaneous transition frequencies are $\omega^1_{v_1v_2v_1'v_2'}$. The frequencies are: $\omega^1_{v_1v_1'}$ has the values $\omega^1_{01} = 0.18$, $\omega^1_{12} = 0.16$, $\omega^1_{23} = 0.14$, $\omega^1_{02} = 0.34$, $\omega^1_{13} = 0.3$; $\omega^2_{v_2v_2'}$ has the values $\omega^2_{02} = 0.11$,

$\omega^2_{12} = 0.1$, $\omega^2_{23} = 0.09$, $\sim \omega^1_{12} = 0.21$, $\omega^1_{13} = 0.19$ in $rad\,fs^{-1}$; $\omega^{12}_{\nu_1\nu_2\nu_1'\nu_2'} = \omega^1_{\nu_1\nu_1'} \pm \omega^2_{\nu_2\nu_2'}$. Thus, total number of frequencies to construct the field is 28 distinct transition frequencies. The transition dipole moments are $\mu^1_{01} = 0.5185$, $\mu^1_{12} = 0.7079$, $\mu^1_{23} = 0.8352$, $\mu^1_{02} = 0.1079$, $\mu^1_{13} = 0.1823$, $\mu^2_{01} = 0.5205$, $\mu^2_{12} = 0.5359$, $\mu^2_{23} = 0.5444$, $\mu^2_{02} = 0.2137$, $\mu^2_{13} = 0.2377$ and with the dual transitions coupled by $\mu^1_{\nu_1\nu_1'} \times \mu^2_{\nu_2\nu_2'}$, all in units of 10^{-30} *C m*. The target time was $T = 4$ ps, the pulse width was $s = 0.75$ ps. Although the field can have 28 distinct frequencies, there is a larger number of transitions allowed in the system.

The three illustrations below demonstrate the scope of what can happen when seeking controlled subspace dynamics under these various conditions. As a reference control case, the closed loop algorithm was run by eliminating extraneous amplitudes and phases without any attempt to confine the dynamics to a reduced subspace. The goal in all the cases is to pump the population from the initial state |0,0> to the final state |3,3>. The weights were chosen as $\beta_1 = 1.0 \times 10^3$ Å$^2 \times V^{-2}$, $\beta_2 = 1.0 \times 10^{-2}$ rad^{-2} and $\beta_3 = 0$. The resultant field drove 92.6% of the population from |0,0> to |3,3> at the target time, $T = 4$ ps. The power spectrum of the field included significant contributions from all 28 transition frequencies. An examination of the populations over the course of the dynamics indicated a highly complex multi pathway mechanism involving the participation of most of the system's 16 states in making the transfer from |0,0> to |3,3>. The population transfer in the reduced four level system, that is |0,0> → |1,1> → |2,2> → |3,3>, with the optimal field shows that only small portion of population transfer on the state |1,1> and no population on the state |3,3>.

The first case of reduced space dynamics involves a subspace consisting of the states |0,0>, |1,1>, |2,2>, |3,3>. With the allowed selection rules those subspace states are only connected in the path |0,0> → |1,1> → |2,2> → |3,3>. Thus, the goal is to transfer population along this path from |0,0> to |3,3> without involving any other states. The initial simulated experiment with this extra goal involved only using the population cost term in Eq. (5d), and the weights were chosen as $\beta_1 = 1.0 \times 10^3$ Å$^2 \times V^{-2}$, $\beta_2 = 1.0 \times 10^{-6}$ rad^{-2}, and $\beta_3 = -1.0 \times 10^{-3}$ fs^{-1}. The term weighted by $\beta_3 < 0$ in Eq. (5d) contained all 4 populations of the states residing inside of the subspace. This case is an example of when the reduced space has dimension $N = 4$ and $N - N' = 12 > N'$. Thus, for reasons of experimental efficiency it would be physically equivalent, and likely best, to use the measured population of the 4 pathway states. The resultant optimal field in Figure 2(a) drove 96.3% of the population from the ground state to the target. Upon examining the power spectrum in Figure 2(b), the |0,0> → |1,1>, |1,1> → |2,2> and |2,2> → |3,3> transitions dominate, as expected for the specified subspace. Figure 2(c) shows the population vector for all of the states over the course of the field's influence.

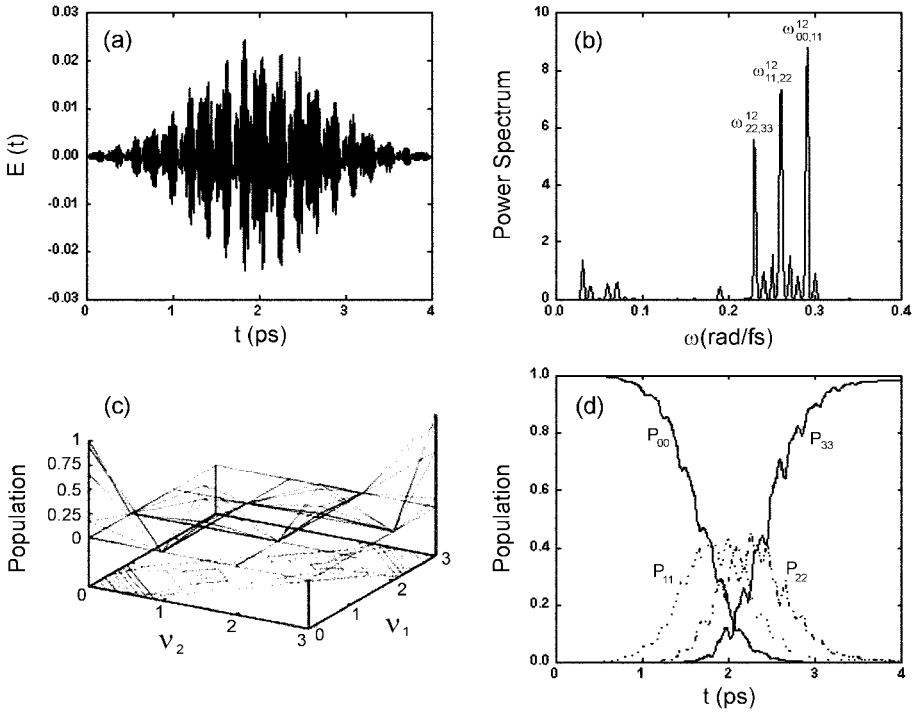

Figure 2. Learning control of a two variable, sixteen state system where the goal is reduced subspace dynamics amongst the states |0,0>, |1,1>, |2,2>, |3,3> for the population transfer |0,0> → |3,3>. The learning control is implemented by placing pressure against population outside of the subspace. (a) The optimal control field found using a cost specifically designed to transfer amplitude along the reduced space pathway |0,0> → |1,1> → |2,2> → |3,3>, (b) the power spectrum of the field with the dominant frequencies labelled as $\omega^{12}_{\nu_1\nu_2,\nu_1'\nu_2'}$, (c) the corresponding time sequence of the population $P_{\nu_1\nu_2}$ contour maps and (d) the population for the reduced four-level system driven by the same optimal control field as a function of time.

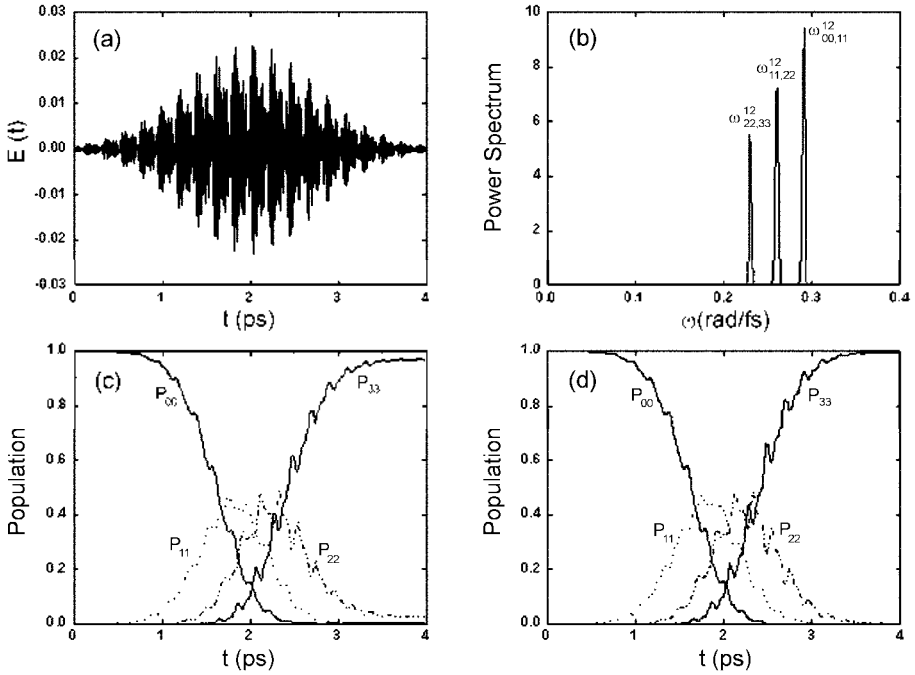

Figure 3. Learning control by filtering algorithm with the same sixteen state system where the goal is the population transfer $|0,0\rangle \rightarrow |3,3\rangle$ by keeping frequencies only corresponding to the states $|0,0\rangle$, $|1,1\rangle$, $|2,2\rangle$, $|3,3\rangle$ instead of the extra cost functional. (a) The optimal control field found using filtering algorithm at every iteration, (b) the power spectrum of the field with the dominant frequencies labelled as $\omega^{12}_{v_1v_2,v_1'v_2'}$, (c) the population $P_{v_1v_2}$ for all sixteen states as a function of time and (d) the population for the reduced four-level system driven by the same optimal control field.

and only significant population occurs in the states $|0,0\rangle$, $|1,1\rangle$, $|2,2\rangle$, $|3,3\rangle$. Application of the same field to the reduced space $N' = 4$ level system produced the population in Figure 2(d) driving 98.5% of population into state $|3,3\rangle$ at the target time. A comparison of Figures 2(c) and 2(d) indicates that the population cost term in Eq. (5d) was quite effective.

As a second approach to attaining reduced space control along the path $|0,0\rangle \rightarrow |1,1\rangle \rightarrow |2,2\rangle \rightarrow |3,3\rangle$, the simulated experiment was repeated by filtering algorithm at every iteration keeping frequencies only corresponding to the states residing inside of the subspace instead of the extra path constraint term in Eq. (5d). The weights were chosen as $\beta_1 = 1.0 \times 10^3$ Å$^2 \times V^{-2}$, $\beta_2 = 1.0 \times 10^{-3}$ rad^{-2}, and $\beta_3 = 0$. The resultant optimal field in Figure 3(a) drove 96.9% of the population from $|0,0\rangle$ to $|3,3\rangle$ at the target time. Power spectrum in Figure 3(b) had only frequencies for the $|0,0\rangle \rightarrow |1,1\rangle$, $|1,1\rangle \rightarrow |2,2\rangle$ and $|2,2\rangle \rightarrow |3,3\rangle$. Figures 3(c) and 3(d) show that the same field applied to the $N' = 4$ set of reduced states produced essentially the same results as with the full space. Filtering is very successful in the present case as the frequencies for the transitions $|0,0\rangle \rightarrow |1,1\rangle$, $|1,1\rangle \rightarrow |2,2\rangle$ and $|2,2\rangle \rightarrow |3,3\rangle$ are sufficiently distinct from all other transition frequencies. The filtering algorithm is simple and attractive, however, it will not be applicable in cases of spectral congestion.

The second example illustrates this point where the transfer of population from $|0,0\rangle$ to $|3,3\rangle$ is sought with the dynamics restricted to a subspace consisting of the $N' = 7$ states $|0,0\rangle$, $|0,1\rangle$, $|0,2\rangle$, $|0,3\rangle$, $|1,3\rangle$, $|2,3\rangle$, $|3,3\rangle$. In this case the selection rules do not imply that the control must sequentially follow these states as set forth. For example, $|0,0\rangle$ and $|0,2\rangle$ are linked by $|0,0\rangle \rightarrow |0,1\rangle \rightarrow |0,2\rangle$ as well as $|0,0\rangle \rightarrow |0,2\rangle$ directly. In this subspace the filtering algorithm will fail as many of the undesirable transitions connecting states inside and outside of the subspace also have the same frequencies necessary for control amongst the seven states forming the subspace. Thus, if successful control within the subspace can be attained in this case, it must employ close cooperation between the field structure and the overall system dynamics possibly employing subtle interference effects. To explore this situation the following weights were used in Eq. (4): $\beta_1 = 1.0 \times 10^3$ Å$^2 \times V^{-2}$, $\beta_2 = 1.0 \times 10^{-6}$ rad^{-2}, and $\beta_3 = -1.0 \times 10^{-3}$ fs^{-1}. The β_3 term contained the population of all seven states inside of the subspace. The resultant field in Figure 4(a) drove 93.9% of the population from the ground state $|0,0\rangle$ to the target $|3,3\rangle$ at the target time. Upon examining the power spectrum in Figure 4(b), the most prominent intensity is $\omega^{12}_{02,13}$ along with lines with significant intensity at the frequencies ω^{1}_{12}, ω^{1}_{23}, ω^{1}_{13}, ω^{2}_{01}, ω^{2}_{12}, and ω^{2}_{02}. Figure 4(c) shows the significant populations over the course of the field's influence, and only sizable population exists in states lying within the subspace. Application of the same field to just the reduced seven level subspace system produced the populations shown in Figure 4(d) where 91.1% of the population is driven from the ground state to the state $|3,3\rangle$. The full mechanism by which the control maintains almost all of the dynamics in the subspace is subtle including the feature that population in the state $|0,3\rangle$ is very small

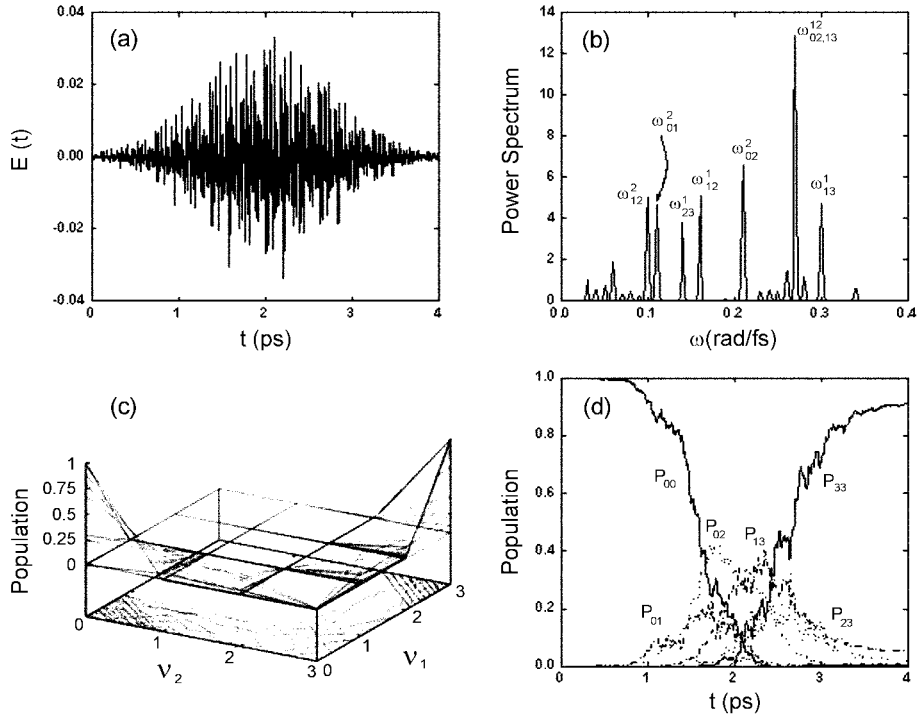

Figure 4. Learning control of a two variable, sixteen state system where the goal is the population transfer |0,0> → |3,3> with the dynamics restricted to a subspace consisting of the $N'' = 7$ states |0,0>, |0,1>, |0,2>, |0,3>, |1,3>, |2,3>, |3,3>. The learning control is implemented by placing pressure against population outside of the subspace. (a) The optimal control field found using a cost specifically designed to confine the dynamics to the reduced states, (b) the power spectrum of the field where the dominant single variable ($\omega^{i}_{v_i v_i'}$ for $i = 1, 2$) and two variable ($\omega^{12}_{v_1 v_2, v_1' v_2'}$) transitions are labelled, (c) the corresponding time sequence of the population $P_{v_1 v_2}$ contour maps and (d) the population for the reduced seven-level system driven by the same optimal control field as a function of time.

throughout the controlled evolution. The close similarity of the population evolution in Figures 4(c) and 4(d) clearly indicates the flow |0,0> → |0,1> → |0,2> → |1,3> → |2,3> → |3,3>, although transitions amongst these states involve both one and two quanta from the spectrum Figure 4(b). Thus, the actual mechanism is likely more complex than the simple population flow would indicate. The success of this case is encouraging for the ability to attain reduced space control in complex multi-level systems possibly even with competing spectral congestion.

Discussion

In this work, we have shown the ability of closed loop quantum learning technique to attain good quality control while steering the dynamics reside within a reduced dimensional space by the tailored cost functional. Specifically designed cost functionals can be manipulated efficiently to steer the dynamics on the most desired subsystem Hamiltonian so that the desired Hamiltonian can be inverted. Both frequency filtering and pressure on the population of states outside of the subspace can be effective for this purpose, with the latter procedure being more flexible. In practice, combined partial spectral filtering and population pressure may form the best means to achieve the dual goals of good target control and dynamical confinement to a subspace. The potential ability to reach the simultaneous goals rests on the fact that generally many controls, and control pathways, may exist giving good yields in the target. Naturally, each case will have its own special features and a proper exploration of this matter must await laboratory implementation of the concept. Attaining reduced space control will call for additional observations when control field frequency filtering alone is not adequate. This extra effort may be well worthwhile for a variety of reasons. First, effective controlled dynamics confined to a subspace has the clear prospect of simplifying the analysis of the control mechanism. Second, applications of controlled dynamics aiming at extracting Hamiltonian information could also beneficially utilize the ability to focus the dynamics into a subspace to simplify the inversion effort.

In general, directing the control to lie in a subspace could also be exploited to avoid physically undesirable dynamics, including states that are especially sensitive to deleterious environment interactions. Future work also needs to explore the ability to confine controlled molecular dynamics to a particular region of configuration space or to the participation of particular chemical moieties in complex polyatomic molecules. Analogous situations may also arise when considering subspaces for controlled electron dynamics in complex solid state devices.

Acknowledgment. This work was supported by the Korea Research Foundation Grant (KRF-2001-005-D22001).

References

1. (a) Peirce, A.; Dahleh, M.; Rabitz, H. *Phys. Rev.* **1988**, *A37*, 4950. (b) Shi, S.; Woody, A.; Rabitz, H. *J. Chem. Phys.* **1988**, *88*, 6870. (c) Shi, S.; Rabitz, H. *J. Chem. Phys.* **1990**, *92*, 364. (d) Judson, R. S.; Lehmann, K. K.; Rabitz, H.; Warren, W. S. *J. Mol. Struct.* **1990**, *223*, 425.
2. Kosloff, R.; Rice, S. A.; Gaspard, P.; Tersigni, S.; Tannor, D. *J. Chem. Phys.* **1989**, *139*, 201.
3. Demiralp, M.; Rabitz, H. *Phys. Rev.* **1998**, *A57*, 2420.
4. (a) Kim, Y. S.; Rabitz, H.; Askar, A.; McManus, J. B. *Phys. Rev.* **1991**, *B44*, 4892. (b) Kim, Y. S.; Tadi, M.; Rabitz, H.; Askar, A.; McManus, J. B. *Phys. Rev.* **1994**, *B50*, 15744. (c) Kim, Y. S.; Rabitz, H.; Tadi, M.; Askar, A.; McManus, J. B. *Int. J. Engng. Sci.* **1995**, *33*, 907.
5. Rabitz, H.; Zhu, W. *Acc. Chem. Res.* **2000**, *33*, 572.
6. (a) Judson, S.; Rabitz, H. *Phys. Rev. Lett.* **1992**, *68*, 1500. (b) Gross, P.; Neuhauser, D.; Rabitz, H. *J. Chem. Phys.* **1993**, *98*, 4557.
7. Goldberg, D. *Genetic Algorithms in Search, Optimization, and Machine Learning*; Addison-Wesley: Reading, MA, 1989.
8. Geremia, J. M.; Zhu, W.; Rabitz, H. *J. Chem. Phys.* **2000**, *113*, 10841.
9. (a) Weinacht, T.; Ahn, J.; Bucksbaum, P. *Natures* **1999**, *397*, 222. (b) White, J.; Bucksbaum, P. *J. Phys. Chem.* **1999**, *103*, 10166.
10. Bardeen, C. J.; Yakovlev, V. V.; Wilson, K. R.; Carpenter, S. D.; Weber, P. M.; Warren, W. S. *Chem. Phys. Lett.* **1997**, *280*, 151.
11. Assion, A.; Baumert, T.; Bergt, M.; Brixner, T.; Kiefer, B.; Seyfried, D.; Strehle, M.; Gerber, G. *Science* **1998**, *282*, 919.
12. Bartels, R. *et al. Nature* **2000**, *406*, 164.
13. Daniel, C. *et al. Chem. Phys.* **2001**, *267*, 247.
14. Meshulach, D.; Silberberg, Y. *Phys. Rev.* **1999**, *A60*, 1287.
15. Hornung, T.; Meier, R.; Motzkus, M. *Chem. Phys. Lett.* **2000**, *326*, 445.
16. Amitay, Z.; Ballard, J.; Stauffer, H.; Leoni, S. *Chem. Phys.* **2001** *267*, 141.
17. Levis, R. J.; Menkir, G.; Rabitz, H. *Science* **2001**, *292*, 709.
18. Kim, H. J.; Kim, Y. S. *Bull. Korean Chem. Soc.* **2001**, *22*, 455.
19. Phan, M. Q.; Rabitz, H. *J. Chem. Phys.* **1999**, *110*, 34.
20. Tang, H.; Kosloff, D.; Rice, S. A. *J. Chem. Phys.* **1996**, *104*, 5457.